A 1:2 Copper(II)–Tripeptide Complex for DNA Binding and Cleavage Agent under Physiological Conditions

by **Pulimamidi R. Reddy***[a]), **Pallerla Manjula**[a]), **Tushar K. Chakraborty**[b]), and **Rajarshi Samanta**[b])

[a]) Department of Chemistry, Osmania University, Hyderabad – 500007, India
(phone: +91-40-27171664; fax: +91-40-27090020; e-mail: rabi_pr@rediffmail.com)
[b]) Indian Institute of Chemical Technology, Hyderabad – 500007, India

A 1:2 copper–tripeptide complex, $[Cu^{II}(Boc\text{-}His\text{-}Gly\text{-}His\text{-}OMe)_2]^{2+}$, was synthesized and structurally characterized. The absorption band at 577 nm suggests a square-planar geometry around Cu^{II}. The DNA-binding and DNA-cleavage properties of the Cu^{II} complex were investigated. The complex binds to calf thymus DNA (CT DNA) in an intercalative fashion and cleaves plasmid pUC-19 DNA hydrolytically at micromolar concentrations under physiological conditions. The intrinsic binding constant ($K_b = 1.2 \times 10^2$ M^{-1}) for the binding of Cu–tripeptide complex with DNA suggests that this complex is suitable for rapid diffusion on the pharmacological time scale.

Introduction. – The field of nucleic acid-targeted drug design has been the subject of several investigations in recent years [1–10]. This is because the DNA-binding proteins such as restriction endonucleases and transcriptional factors recognize specific DNA sequences to carry out the precise genetic manipulations ongoing in a living system. Low-molecular-weight bioactive ligands, which also recognize and interact with DNA, are of chemical, biological, and medical significance as potential artificial gene regulators or cancer chemotherapeutic agents. The remarkable biological potencies of these bioactive ligands are thought to be a consequence of their ability to bind to cellular DNA, and produce single or double stranded breaks with great efficiency.

Metallopeptides are unique among metal-based nucleic acid-binding agents in their ability to incorporate and position along the periphery of a well-defined metal-complex framework the same chemical functional groups used by proteins and peptide-based natural product antitumor agents for the molecular recognition of DNA and RNA [11]. Metallopeptides of the general form Cu^{II}- or Ni^{II}(Gly-Gly-His) have contributed to our understanding of fundamental nucleic acid recognition and reactivity phenomena in the context of both proteins and low-molecular-weight agents [12]. Our laboratory has been involved in the development of nucleic acid-targeted drug design under physiological conditions [13–16]. Here, we report the synthesis and characterization of the complex $[Cu^{II}(Boc\text{-}His\text{-}Gly\text{-}His\text{-}OMe)_2]^{2+}$ (*Scheme*) along with its DNA-binding and DNA-cleavage properties. The Cu complex binds to DNA in an intercalation mode ($K_b = 1.2 \times 10^2$ M^{-1}) and converts supercoiled plasmid pUC-19 DNA into a nicked circular form at micromolar concentration.

Results and Discussion. – *Characterization of the Complex.* The IR spectra of the Cu complex indicating the coordination of the 1*H*-imidazole N-atom with the metal,

Scheme

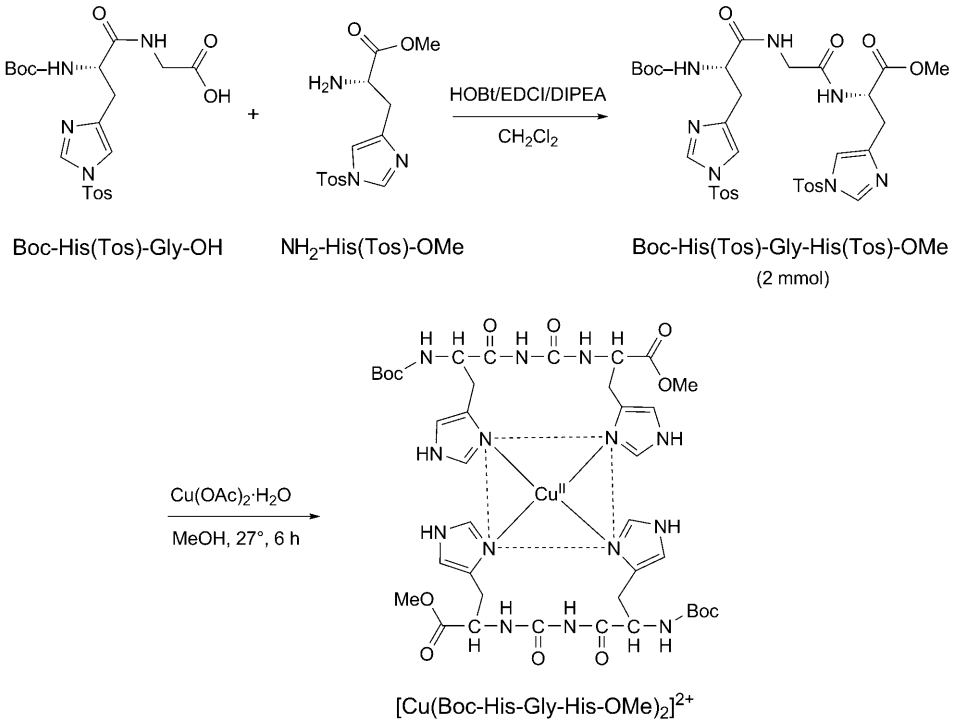

and the appearance of a new band at 568 cm^{-1} confirms the N-atom ligation around Cu. ESI Mass spectra were utilized to identify the composition of the Cu complex (*Fig. 1*). The molecular-ion peak at *m/z* 512 ($[M+NH_4]^+$) confirms the 2:1 peptide–Cu complex. Accordingly, N(4) ligation around Cu has been proposed (*Fig. 2*).

The UV profile of CT DNA at a fixed concentration and increasing concentrations of the Cu complex was monitored at 260 nm in *Tris*·HCl buffer (pH 7.5). In the absence of DNA, no significant absorbance was observed in the range of 240–280 nm, neither for the free peptide nor for the complex $[Cu^{II}(tripeptide)_2]$. However, an increase in UV absorbance was observed on the addition of the Cu complex to CT DNA (*Fig. 3*,*a*). The absorption maximum (λ_{max}) of CT DNA was also shifted from 257 to 253 nm. This indicates the denaturation or a conformational change of the DNA duplex.

The thermal denaturation profile of DNA in the absence and presence of the Cu complex is provided in *Fig. 3*,*b*. A slight increase of 3–4° was observed in the T_m profile of the complex as compared to free DNA. As it is well-known, the increase of T_m means an intercalative and/or phosphate binding, whereas a decrease is an indicator of binding to the bases. These results provide an evidence for intercalative and/or phosphate binding of the Cu^{II} complex with DNA. It seems that the first interaction of DNA with the complex is due to an electrostatic interaction between the positively charged

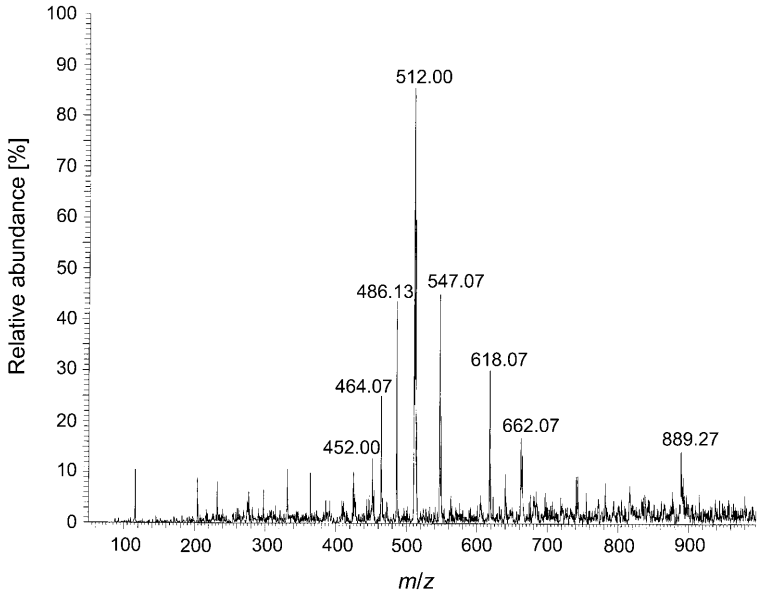

Fig. 1. *ESI Mass spectrum of the Cu complex*

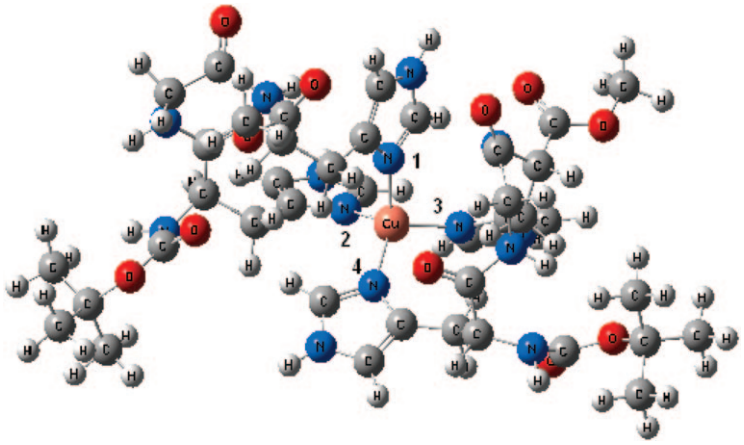

Fig. 2. *Energy-minimized molecular structure of* $[Cu^{II}(Boc\text{-}His\text{-}Gly\text{-}His\text{-}OMe)_2]^{2+}$. Optimized calculated bond lengths (in Å) and bond angles (in degrees) of Cu and the interacting N-atoms: Cu–N(1) 1.922, Cu–N(2) 1.947, Cu–N(3) 1.945, Cu–N(4) 1.936, Cu–N(1)–N(2) 100.9, Cu–N(1)–N(3) 104.5, Cu–N(1)–N(4) 115.4.

complex and the negatively charged DNA phosphate backbone. This is followed by an intercalative mode of binding.

Ethidium bromide (EB) emits intense fluorescence light in the presence of DNA due to its strong intercalation between the adjacent DNA base pairs. It was reported that the enhanced fluorescence can be quenched by the addition of a second molecule

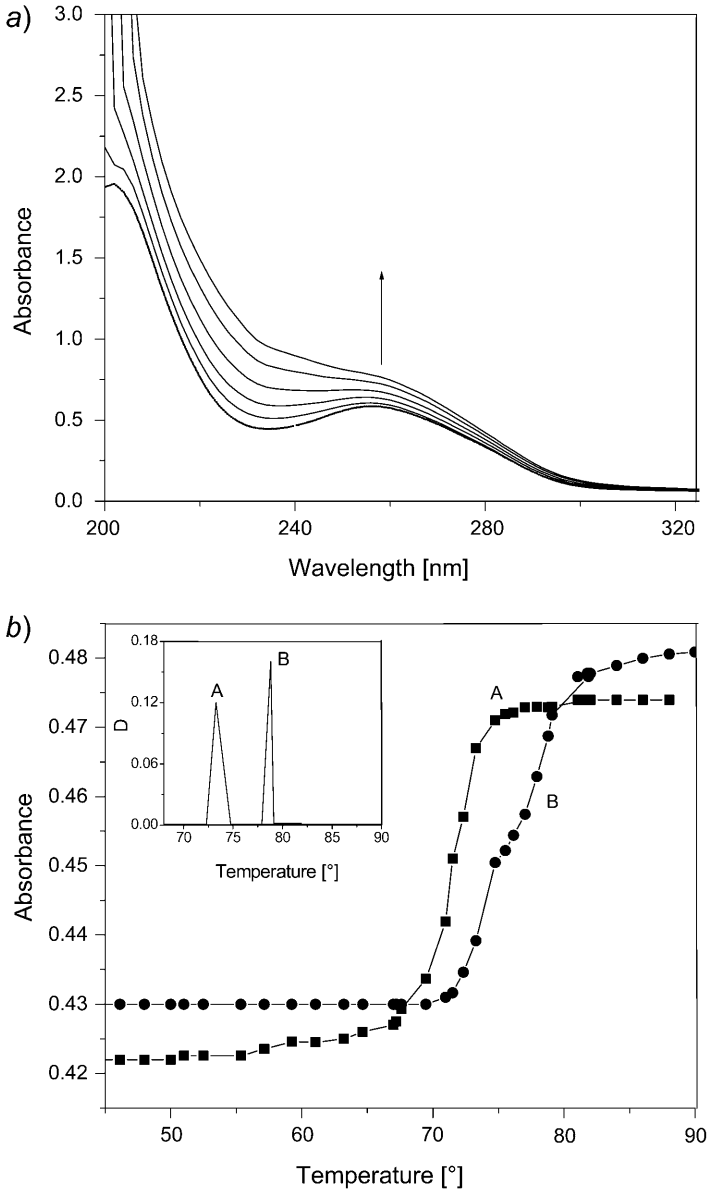

Fig. 3. a) *UV/VIS Absorption spectra of* $[Cu^{II}(Boc\text{-}His\text{-}Gly\text{-}His\text{-}OMe)_2]^{2+}$ *in the absence* (bottom) *and presence* (top) *of increasing amounts of the complex*. b) *Thermal denaturation profile and differential melting curves* (*inset*) *of calf thymus DNA* (75 μM) *before* (*A*) *and after* (*B*) *addition of Cu complex* (75 μM). D is the difference in absorbance.

[17][18]. The quenching extent of EB fluorescence bound to DNA was used to determine the extent of binding between the second molecule and DNA. The emission

spectra of EB bound to CT DNA in the absence and the presence of the Cu^{II} complex is given in *Fig. 4,a*. The addition of the Cu^{II} complex to DNA pretreated with EB caused appreciable reduction in emission intensity, indicating that the complex competes with EB in binding to DNA.

According to the *Stern–Volmer* equation [18]:

$$I_0/I = 1 + K_{sq} \cdot r$$

where I_0 and I are the fluorescence intensities in the absence and the presence of complex, respectively, K_{sq} is a linear *Stern–Volmer* quenching constant dependent on the ratio of the concentrations of bound EB to unbound EB, and r is the concentration ratio of the complex to DNA. The quenching plot (*Fig. 4,a*) illustrates that the quenching of EB bound to DNA by the Cu^{II} complex is in good agreement with the linear *Stern–Volmer* equation, which indicates that the complex binds to DNA. In the plot of I_0/I *vs.* [complex]/[DNA], K_{sq} is given by the ratio of slope to intercept, and the K_{sq} value for the Cu^{II} complex is 0.14.

Fluorescence *Scatchard* plots for the binding of EB to CT DNA in the presence of the Cu complex were obtained as described by *Lepecq* and *Paoletti* [19]. The binding isotherms of EB and DNA in the absence and presence of the complex were determined experimentally and presented in *Fig. 4,b*. The *Scatchard* plots in the presence of the complex result in the decrease of slope as compared to the complex free plot, with no change in the intercept (*Fig. 4,b*). These results confirm an intercalative binding of the Cu^{II} complex with DNA [19].

The cleavage reaction on supercoiled pUC-19 DNA was monitored by agarose-gel electrophoresis. When supercoiled DNA was subjected to electrophoresis, a relatively fast migration was observed for the intact supercoiled DNA (Form I). If scission occurs on one strand (nicking), the supercoiled DNA will relax to generate a slower-moving open circular form (Form II). If both strands are cleaved, a linear form (Form III) that migrates between Form I and Form II will be generated. When supercoiled pUC-19 DNA was incubated at 37° for 4 h in 5 mM *Tris*·HCl/5 mM NaCl at pH 7.5 in the presence of Cu complex, it was converted from supercoiled (Form I) to nicked circular form (Form II; *Fig. 5,a*). Although this complex did not require the addition of an external agent, we were keen to discount the possibility that the DNA cleavage occurred *via* an OH radical-based depurination pathway. When supercoiled pUC-19 DNA was incubated with higher amounts of the Cu complex in the presence of DMSO or glycerol, no significant change in the cleavage was observed. This clearly indicates that this complex-mediated cleavage in the absence of exogenous coreactants does not proceed *via* either diffusible OH radicals or free superoxide [20].

The cleavage of pUC-19 DNA by the Cu complex has been kinetically characterized by quantification of supercoiled and nicked DNA. The observed distribution of supercoiled and nicked DNA in an agarose gel provides a measure of the extent of hydrolysis of the phosphodiester bonds in each plasmid DNA, and the data were used to perform a simple kinetic analysis. *Fig. 5,b*, shows the time-course plot for the decrease of Form I and formation of Form II during the reaction under mild conditions by the Cu complex. The decrease of Form I fits well to a single exponential decay curve, and the increase of Form II also fits well to a single exponential curve.

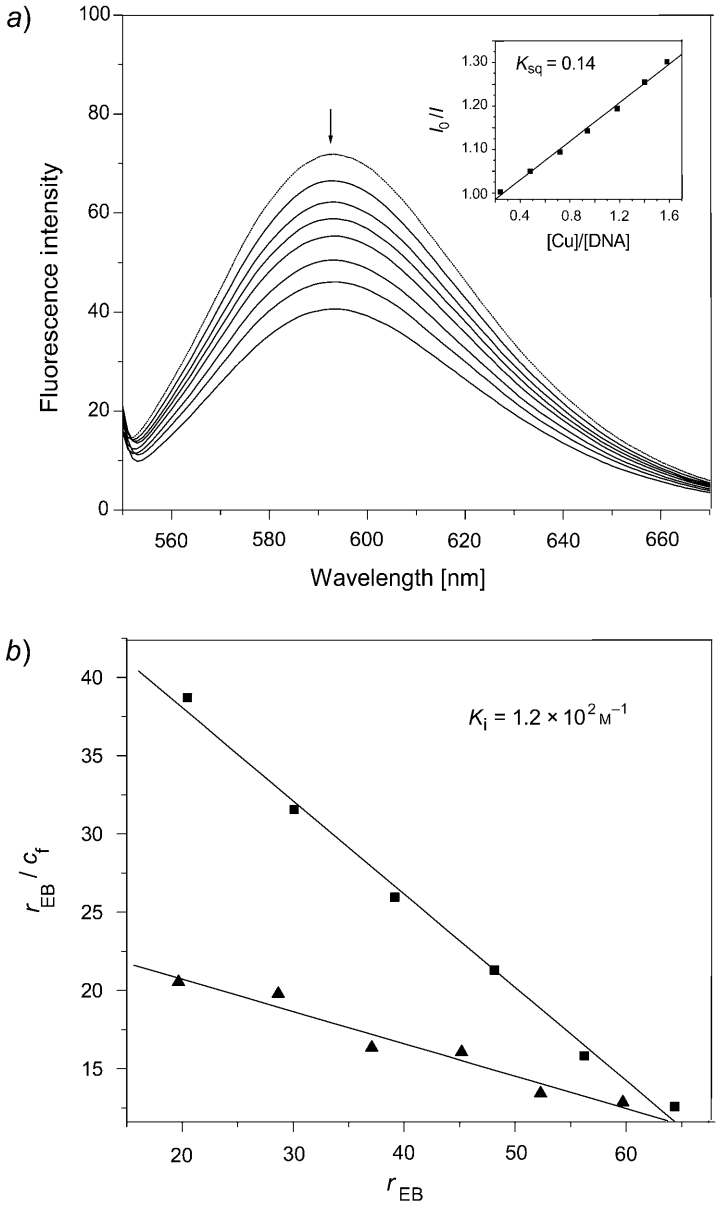

Fig. 4. a) *Fluorescence emission spectra of ethidium bromide* (EB) *bound to CT DNA in the absence* (top) *and presence* (bottom) *of 1:2 Cu^{II}–tripeptide complex*. [Complex]/[DNA] = 0, 0.24, 0.48, 0.72, 0.94, 1.18; λ_{ex} = 540 nm. Inset: *Stern–Volmer* quenching plot. b) *Fluorescence* Scatchard *plots for the binding of EB to CT DNA in the absence* (■) *and presence* (▲) *of [Cu^{II}(Boc-His-Gly-His-OMe)$_2$]$^{2+}$*. The term r_{EB} is the concentration ratio of bound EB to total DNA, and c_f is the concentration of free EB.

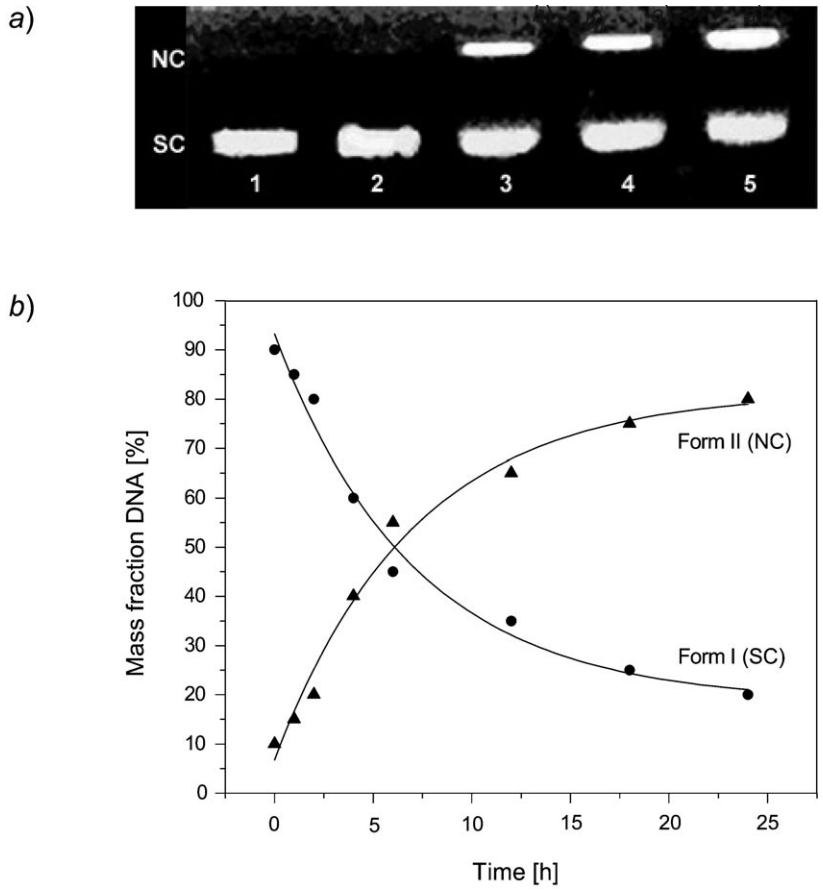

Fig. 5. a) *Agarose-gel electrophoresis patterns for the cleavage of pUC-19 DNA by the Cu complex. Lane 1:* DNA control; *Lanes 2–5:* [Cu complex] = 125, 250, 350, 500 μM, resp. NC is the nicked circular and SC the supercoiled form of pUC-19 DNA, resp. b) *Disappearance of supercoiled* (●, Form I) *and formation of nicked circular* (▲, Form II) *forms of plasmid DNA in the presence of Cu complex* (250 μM) *as a function of the incubation time* (pH 7.5, temp. 37°).

From these curve fits, the hydrolysis rate constants at 37° and at a complex concentration of 250 μM were determined to be 2.82×10^{-5} s^{-1} ($R = 0.979$) for the Cu complex.

Recently, *Long* and co-workers [21] have shown by NMR and molecular-simulation model studies that Ni^{II}(Gly-Gly-His) (1:1 complex) binds to DNA through minor-groove contacts, and established that it acts as a mini model for minor-groove binding. The $[Cu^{II}(Boc\text{-}His\text{-}Gly\text{-}His\text{-}OMe)_2]^{2+}$ complex with a square-planar geometry perfectly fits into the model suggested by them. In their complex, the DNA contacts are through His NH, terminal amine N–H H-atoms, and H-bond formation through the AT region, whereas in our complex the contacts are most likely through imidazole NH H-atoms.

It was observed recently [2] that the DNA binding constant below 10^4 M^{-1} was assumed to allow a sufficiently rapid diffusion on the pharmacological time scale, and even moderate values of DNA binding (10^5–10^6 M^{-1}) can limit diffusion. With a K_b value of 1.2×10^2 M^{-1} along with its cleavage ability, the complex [Cu^{II}(Boc-His-Gly-His-OMe)$_2$]$^{2+}$ has a potential to be developed as a nucleic acid-targeted drug.

The authors thank the *University Grants Commission* (New Delhi) and the *Department of Science and Technology* (Government of India) for financial support.

Experimental Part

General. Boc-NH-His(Tos)-Gly-OH, NH_2-His(Tos)-OMe, and ethidium bromide (EB; 99.99% purity) were obtained from *Sigma* (Germany). $Cu(OAc)_2 \cdot H_2O$ (*AnalaR* grade) was purchased from *Merck*. All other chemicals and solvents (spectroscopic grade) were purchased from commercial sources and used without further purification. Doubly dist. H_2O was used to prepare the buffer solns. Calf thymus (CT) DNA was obtained from *Fluka* (Switzerland). Plasmid pUC-19 DNA, agarose gel, and *Tris*·HCl (*Tris* = Tris(hydroxymethyl)aminomethane) buffer were obtained from *Bangalore Genei* (India). The spectroscopic titrations were carried out in aerated buffer (5 mM *Tris*·HCl, 50 mM NaCl, pH 7.5) at r.t. Molar conductivity: *Digisun DI-909* digital conductivity bridge with a dip-type cell, using a 10^{-3} M soln. of the complex in MeOH. Magnetic susceptibility: *Faraday* balance (*CAHN-7600*) at r.t. using $Hg[Co(CNS)_4]$ as standard. Diamagnetic corrections were made by using *Pascal*'s constants [22]. EPR Spectra: *Jeol* (*JES-FA200*) X-band spectrometer. UV/VIS Spectra: *Shimadzu 160A* spectrophotometer (800–200 nm); λ_{max} in nm. IR Spectra: *Perkin-Elmer* FT IR spectrometer; KBr pellets, $\tilde{\nu}$ in cm^{-1}. ^{1}H-NMR Spectra: *Varian Gemini* FT-NMR spectrometer at 200 MHz in $CDCl_3$. ESI-MS: *Micro Mass quattro Lc* triple-quadrupole mass spectrometer with MassLynx software (Manchester, UK); in *m*/*z*. Elemental analyses: *Heraeus Carlo Erba 1108* elemental analyzer. Cu Content: *Perkin-Elmer 2380* atomic absorption spectrometer.

Peptide Synthesis. For the synthesis of the tripeptide Boc-NH-His(Tos)-Gly-His(Tos)-OMe ($C_{34}H_{42}N_7O_{10}S_2$), the procedure of *Varenkamp* and co-workers [23] was applied. To a soln. of Boc-NH-His(Tos)-Gly-OH in anh. CH_2Cl_2 at 0° under N_2, 1-hydroxybenzotriazole (HOBt) was added under stirring, followed by 1-ethyl-3-(3-(dimethylamino)propyl)carbodiimide hydrochloride (EDCl). After 15 min at 0°, NH_2-His(Tos)-OMe (dissolved in CH_2Cl_2 and neutralized with $EtN(i\text{-}Pr)_2$) was added to the mixture, which was allowed to reach r.t., and stirring was continued for 6 h. The reaction was quenched with a sat. aq. NH_4Cl soln. and extracted with AcOEt. The combined org. layers were washed with a sat. aq. NH_4Cl soln., sat. aq. $NaHCO_3$ soln., and brine, dried (Na_2SO_4), and evaporated *in vacuo*. The residue was purified by CC (SiO_2 (60–120 μm); $CHCl_3$/MeOH). IR (KBr): 3407*m* (N–H), 1670*s* (CO–N), 1750*w* (COOR), 1080 (imidazole N). ^{1}H-NMR (200 MHz, $CDCl_3$): 8.10–7.04 (*m*, 14 H); 5.68 (*d*, *J* = 7.5, 1 H); 4.92–4.69 (*m*, 1 H); 4.53–4.34 (*m*, 1 H); 3.97–3.78 (*m*, 2 H); 3.66 (*s*, 3 H); 3.19–2.89 (*m*, 4 H); 2.43 (*s*, 6 H); 1.42 (*s*, 9 H). ESI-MS: 773 ([*M* + H]$^+$). Anal. calc. for $C_{34}H_{42}N_7O_{10}S_2$: C 56.50, H 5.81, N 13.57; found: C 56.49, H 5.45, N 13.58.

Synthesis of the Metal Complex. A soln. of Boc-NH-His(Tos)-Gly-His(Tos)-OMe (140 mg, 0.181 mmol) in anh. MeOH (10 ml) was stirred for 1 h. Then, the pH of the soln. was adjusted to *ca.* 7.0 with Et_3N. To this soln., $Cu(OAc)_2 \cdot H_2O$ (19 mg, 0.0906 mmol) in MeOH was added, and stirring was continued for 6 h. The resulting green colored precipitate was filtered off, washed with hot MeOH, and dried to afford the Cu complex (*Scheme*). Yield: 50%. Λ_m (Molar conductance) 1.20×10^{-3} Ω^{-1} cm^2 mol^{-1}. M.p. 240°. UV/VIS (MeOH): 577. IR (KBr): 3446*m* (N–H), 1684*s* (CO–N), 1756*w* (COOR), 1122 (imidazole N), 568 (Cu–N). ESI-MS: 512 ([2 *M* + NH_4]$^+$). Anal. calc. for $C_{40}H_{58}N_{14}O_{12}Cu$: C 48.53, H 5.86, N 19.81, Cu 6.42; found: C 48.50, H 5.83, N 19.82, Cu 6.45.

DNA Binding. Preparation of a CT DNA Soln. A conc. CT DNA stock soln. was prepared in 5 mM *Tris*·HCl/50 mM NaCl in H_2O at pH 7.5, and the concentration of the DNA soln. was determined by UV absorbance at 260 nm. The molar absorption coefficient was taken as 6600 M^{-1} cm^{-1} [24]. The soln. of CT DNA in 5 mM *Tris*·HCl/50 mM NaCl (pH 7.5) gave a ratio of UV absorption at 260 and 280 nm, A_{260}/A_{280},

of *ca*. 1.8–1.9, indicating that the DNA was sufficiently free of protein [25]. All stock solns. were stored at 4° and used within one week. The concentration of EB was determined spectrophotometrically at 480 nm ($\varepsilon = 5680\ \text{M}^{-1}\text{cm}^{-1}$) [26].

Absorption-Spectroscopic Studies. Absorption spectra were recorded on a *Jasco V-530* UV/VIS spectrophotometer using 1-cm quartz microcuvettes. Increasing known amounts of the Cu complex in MeOH was added to DNA. The experiments were carried out at r.t. in 5 mM *Tris*·HCl/50 mM NaCl (pH 7.5). After each addition, the mixture was shaken and kept for *ca*. 5 min, and the absorbance was recorded.

Thermal-Denaturation Studies. Thermal-denaturation studies were recorded on a *Shimadzu 160A* spectrophotometer equipped with a thermostated cell holder. DNA (75 μM) was treated with the complex (75 μM) in buffer (5 mM *Tris*·HCl/50 mM NaCl) at pH 7.5. The samples were continuously heated at a rate of 1°/min, while the absorption changes at 260 nm were monitored. Values for the melting temperature (T_m) and for the melting interval (ΔT) were determined according to the procedures reported in [27]. Differential melting curves were obtained by numerical differentiation of the experimental melting curves.

Intercalator Displacement by Fluorescence Spectroscopy. Fluorescence spectra were recorded with a *SPEX- Fluorolog 0.22 m* fluorimeter equipped with a 450-W Xe lamp. The slit widths were $2 \times 2 \times 2 \times 2$, and the emission spectral range was 550–650 nm. All fluorescence titrations were carried out in 5 mM *Tris*·HCl/50 mM NaCl (pH 7.5) at r.t. The soln. containing DNA and EB was titrated with varying concentrations of the Cu^{II} complex. The solns. were excited at 540 nm, and the fluorescence emission, which corresponds to 565 nm, was recorded. The samples were shaken and kept for 2–3 min for equilibrium, and then the spectra were recorded. The DNA concentration was always 54 μM. The concentrations of the complex was in the range of 0–77 μM, and the EB concentration was 43 μM.

Fluorescence spectra were also used to obtain *Scatchard* plots. For these, titrations of DNA against EB in the absence and presence of the Cu^{II} complex was performed. Initial concentration of DNA in 5 mM *Tris*·HCl/50 mM NaCl was 34 μM. After each addition of EB to the solns. containing DNA and the metal complex, the emission spectra were recorded from 550 to 650 nm with 540-nm excitation at r.t. Corrections were made for the volume changes during the course of titrations. The data were analyzed by the method of *Lepecq* and *Paoletti* [19] to obtain bound (c_b) and free (c_f) concentrations of EB. *Scatchard* plots were obtained by plotting r_{EB}/c_f *vs.* r_{EB} (where $r_{EB} = c_b/[\text{DNA}]$).

Electrophoresis Experiments. Agar-gel electrophoresis was performed with pUC-19 DNA in *Tris*·HCl buffered solns. at pH 7.5. DNA-Cleavage studies were performed by adding varying concentrations of the Cu^{II} complex (0–500 μM) to 2 μl of pUC-19 DNA (0.5 μg/μl; 10 mM *Tris*·HCl, 1 mM EDTA, pH 8.0) to 5 mM *Tris*·HCl/50 mM NaCl (total volume 16 μl). After mixing, the DNA solns. were incubated at 37° for 4 h. Kinetic analysis was carried out at fixed concentrations of DNA and Cu^{II} complex with different incubation times under identical experimental conditions. The reactions were quenched by the addition of bromophenol blue and the mixtures were analyzed. Experiments were carried out with 1% agar gels run at 50 V for 4 h in TAE (*Tris*/AcOH/EDTA) buffer. The gels were stained with EB (0.5 μg/ml) and photographed under UV light.

REFERENCES

[1] F. Mancin, P. Tecilla, *New J. Chem*. **2007**, *31*, 800.
[2] J. Sebestik, I. Stibor, J. Hlavacek, *J. Pept. Sci*. **2006**, *12*, 472.
[3] J. L. Czlapinski, T. L. Sheppard, *Chem. Commun.* **2004**, 2468.
[4] T. A. van den Berg, B. L. Feringa, G. Roelfes, *Chem. Commun*. **2007**, 180.
[5] Y. An, Y.-Y. Lin, H. Wang, H.-Z. Sun, M.-L. Tong, L.-N. Ji, Z.-W. Mao, *Dalton Trans.* **2007**, 1250.
[6] W.-J. Mei, Y.-J. Liu, N. Wang, Y.-Z. Ma, H. Wang, L.-Q. Luo, S.-L. Huang, *Transition Met. Chem.* **2006**, *31*, 1024.
[7] J.-L. Tian, L. Feng, W. Gu, G.-J. Xu, S.-P. Yan, D.-Z. Liao, Z.-H. Jiang, P. Cheng, *J. Inorg. Biochem*. **2007**, *101*, 196.
[8] X.-L.Wang, H. Chao, B. Peng, L.-N. Ji, J. Zhang, *Transition Met. Chem*. **2007**, *32*, 125.

[9] J. Chen, X. Wang, Y. Shao, J. Zhu, Y. Zhu, Y. Li, Q. Xu, Z. Guo, *Inorg. Chem*. **2007**, *46*, 3306.
[10] K. Dhara, J. Ratha, M. Manassero, X.-Y. Wang, S. Gao, P. Banerjee, *J. Inorg. Biochem*. **2007**, *101*, 95.
[11] T. A. Steitz, *Q. Rev. Biophys.* **1990**, *23*, 205; C. Zimmer, U. Wähnert, *Prog. Biophys. Mol. Biol*. **1986**, *47*, 31.
[12] E. C. Long, C. A. Claussen, in 'DNA and RNA Binders, From Small Molecules to Drugs', Eds. M. Demeunynk, C. Bailly, W. D. Wilson, John Wiley & Sons, New York, 2003, p. 88.
[13] P. R. Reddy, P. Manjula, S. K. Mohan, *Chem. Biodiversity* **2005**, *2*, 1338.
[14] P. R. Reddy, K. S. Rao, *Chem. Biodiversity* **2006**, *3*, 231.
[15] P. R. Reddy, S. K. Mohan, P. Manjula, T. K. Chakraborty, *Chem. Biodiversity* **2006**, *3*, 456.
[16] P. R. Reddy, K. S. Rao, B. Satyanarayana, *Tetrahedron Lett.* **2006**, *47*, 7311.
[17] B. C. Baguley, M. Le Bret, *Biochemistry* **1984**, *23*, 937.
[18] J. R. Lakowicz, G. Webber, *Biochemistry* **1973**, *12*, 4161.
[19] J.-B. Lepecq, C. Paoletti, *J. Mol. Biol*. **1967**, *27*, 87.
[20] R. Ren, P. Yang, W. Zheng, Z. Hua, *Inorg. Chem*. **2000**, *39*, 5454.
[21] Y.-Y. Fang, B. D. Ray, C. A. Claussen, K. B. Lipkowitz, E. C. Long, *J. Am. Chem. Soc*. **2004**, *126*, 5403.
[22] B. N. Figgis, J. Lewis, 'Modern Coordination Chemistry', Eds. J. Lewis, R. C. Wilkinson, Wiley Interscience, New York, 1967, p. 403.
[23] M. Forster, I. Brasack, A.-K. Duhme, H.-F. Nolting, H. Vahrenkamp, *Chem. Ber*. **1996**, *129*, 347.
[24] J. Murmer, *J. Mol. Biol*. **1961**, *3*, 208.
[25] M. E. Reichmann, S. A. Rice, C. A. Thomas, P. Doty, *J. Am. Chem. Soc*. **1954**, *76*, 3047.
[26] F. Garland, D. E. Graves, L. W. Yielding, H. C. Cheung, *Biochemistry* **1980**, *19*, 3221.
[27] W. D. Wilson, F. A. Tanious, M. Fernandez-Saiz, C. T. Rigl, in 'Methods in Molecular Biology', Vol. 90, Ed. K. R. Fox, Humana Press, Clifton, NJ, 1997.

Received February 24, 2008